Total charge-changing and partial cross-section measurements in the reactions of ~110–250 MeV/nucleon ^{12}C in carbon, paraffin, and water

A. N. Golovchenko,[1] J. Skvarč,[2] N. Yasuda,[3] M. Giacomelli,[2] S. P. Tretyakova,[1] R. Ilić,[2,4] R. Bimbot,[5] M. Toulemonde,[6] and T. Murakami[7]

[1]*Joint Institute for Nuclear Research, 141980 Dubna, Russia*
[2]*J. Stefan Institute, Jamova 39, 1001 Ljubljana, Slovenia*
[3]*International Space Radiation Laboratory, National Institute of Radiological Sciences, 4-9-1 Anagawa, Inage-ku, Chiba 263-8555, Japan*
[4]*Faculty of Civil Engineering, University of Maribor, Smetanova 17, 2000 Maribor, Slovenia*
[5]*Institut de Physique Nucléaire, 91406 Orsay Cedex, France*
[6]*Centre Inter-disciplinaire de Recherches Ion Laser, CIRIL, BP 5133, 14070 Caen Cedex 5, France*
[7]*Division of Accelerator Physics and Engineering, National Institute of Radiological Sciences, 4-9-1 Anagawa, Inage-ku, Chiba 263-8555, Japan*

(Received 26 February 2002; published 17 July 2002)

Total charge-changing cross sections and cross sections for the production of B and Be fragments were directly measured for reactions induced by ~110–250 MeV/nucleon ^{12}C ions in C, CH_2, and H_2O targets. Etched track detector (CR-3) was used, together with an automatic track measuring system and a track matching algorithm, to count and to identify the primary and secondary particles. A comparison of the present data and of previously measured cross sections with model predictions is carried out. For the total charge-changing cross section, a model developed at NASA gives the best agreement with the present results (about 3% on the average). However, for the production of fragments, the results of models deviate on average for all systems studied by 9–58 % from the data presented in this work for $Z=5$ and by 5–47 % for $Z=4$. The model known as NUCFRG2 is the most reliable in giving the closest values for fragmentation cross sections, 9 and 5% for B and Be fragments, respectively, for the systems studied in this work.

DOI: 10.1103/PhysRevC.66.014609 PACS number(s): 25.70.Mn, 25.75.−q

I. INTRODUCTION

A precise knowledge of ion beam transport in matter is of great interest in many aspects of fundamental and applied science. One basic value is the total charge-changing cross section (σ_{TCC}) that is dominated by the total cross section (σ_{T}) and is defined as

$$\sigma_{\mathrm{TCC}}=\sigma_{\mathrm{T}}-\sigma_{\mathrm{el}}-\sigma_{\mathrm{nr}}, \tag{1}$$

where σ_{el} is the elastic cross section and σ_{nr} is the neutron-removal cross section. The total reaction cross section is $\sigma_{\mathrm{R}}=\sigma_{\mathrm{T}}-\sigma_{\mathrm{el}}$. Another basic parameter is the partial cross section (σ_{PCC}) for the production of projectilelike fragments. These fragments carry a lower nuclear charge than the primary beam, but have nearly the same velocity. Knowledge of σ_{TCC} and σ_{PCC} with good accuracy is essential for many research areas including astrophysics, cosmic ray propagation, radiation protection of man in space [1,2], and clinical treatment of cancer [3,4]. However, there are still significant discrepancies between the cross sections predicted by models and experimental data. Carbon ions are one of the most abundant components in galactic cosmic rays and they play a special role in radiation therapy which is currently performed in the clinical centers of Gesellschaft für Schwerionenforschchung (Darmstadt, Germany) and the National Institute of Radiological Sciences (NIRS, Chiba, Japan). In this paper experimental results for total and partial charge-changing cross sections obtained for incident ^{12}C ions at ~110–250 MeV/nucleon and targets made of carbon, paraffin, and water are presented. These results were compared with the data available from previous measurements and model predictions.

II. EXPERIMENTS

Three stacks made of CR-39 track-etch detector (Intercast, Parma, Italy) and thick carbon, paraffin, and water targets were perpendicularly exposed to a ^{12}C beam of initial energy of 275 MeV/nucleon in the biology port of the HIMAC facility (NIRS). Each stack corresponded to a given target material (C, CH_2, and H_2O). The water targets were closed cells made of 3 mm thick Plexiglass walls on the external sides of which two detector plates were glued. One wall had a small hole into which distilled water was injected by a syringe. Table I shows in detail the energy intervals and thicknesses of the targets used in the present work (E_{in} and E_{out} denote the energies of carbon particles calculated in front of and behind a specific target). The detector plates were ~600 μm in thickness interleaved with the targets. Both the detectors and the targets were $\sim 4\times 4$ cm^2 in area. One detector plate was placed in front of the stack to monitor the primary beam and the accompanying particles (produced in materials preceding the stack). The fragments produced in the targets were measured all along the stacks, together with the primary ions and accompanying particles. In fact, two detector plates were put in between neighboring targets to increase the accuracy of track measurements. The number of measured particles impinging on the stack was $\sim 3\times 10^4$ dispersed over the active detector area of ~10 cm^2. Chemical

TABLE I. Energy intervals and thicknesses of targets used in the present work.

C+C		C+CH_2		C+H_2O	
$E_{in}-E_{out}$ (MeV/nucleon)	Target thickness (mm)	$E_{in}-E_{out}$ (MeV/nucleon)	Target thickness (mm)	$E_{in}-E_{out}$ (MeV/nucleon)	Target thickness (mm)
274–234	21.0	274–222	44.0	274–208	55.0
234–190	20.5	248–192	44.0	205–145	40.0
212–136	31.3	221–159	43.7	143–83	30.0
146–78	20.7	191–121	43.9		
		158–70	43.7		

etching (7 M NaOH, 80°C, 14 h) was applied to the detector sheets to develop latent tracks. Then the tracks were scanned by a microscope connected to an automatic measuring system [5]. After automatic counting and measurement of the parameters of the tracks (including the average brightness, positions on the detector sheet, minor and major axes, etc.) the tracks originating from primary and secondary particles were matched [6] on the upper and bottom surface of each detector sheet. This procedure allowed us to exclude from the subsequent analysis unwanted events like bubbles, possible targetlike fragments, radon-induced tracks, and primary particles that underwent fragmentation in materials preceding the stack and in the body of the detector. In such an experiment and for the energy interval covered ($\sim$110–250 MeV/nucleon) the charge resolution (1σ) varied from less than 0.1–0.3 elementary charge units, depending on the particle detected (primary or secondary) and on its penetration depth in the body of the stack. The higher the charge of the particle and the shorter its penetration depth the better is the resolution and vice versa. Figures 1 and 2 show typical spectra of tracks measured after carbon ions passed through a 2.2 cm thick paraffin and a 5.5 cm thick water target, respectively. The energy losses and ranges of primaries and fragments could not be directly measured in this experiment. Therefore, they were calculated using a code after Benton and Henke [7] which was found to be accurate enough for carbon ions [8].

III. RESULTS

A. Total charge-changing cross sections

The total charge-changing cross sections σ_{TCC} were obtained from the numbers of matched tracks corresponding to the peaks of carbon, measured in the active detector areas in front of ($N_{C,\,in}$) and behind ($N_{C,\,out}$) a given target. The conventional exponential function is valid for the systems studied here with good accuracy, and is given as (see also Appendix A)

$$N_{C,\,out}=N_{C,\,in}e^{-(N_A\rho\sigma_{TCC}x)/M}, \tag{2}$$

where N_A, ρ, x, and M are, respectively, the Avogadro number, the density and the thickness of the target, and its atomic or molecular mass. That is in the case of C target the cross section is per nucleus and that for CH_2 and H_2O targets is per molecule. The total charge-changing cross section is easily derived from Eq. (2). Figures 3 and 4 present the general behavior of the total charge-changing cross sections ($\sigma_{TCC,\,exp}$) obtained in this work in comparison with previous experimental results [9–13] for all the systems studied

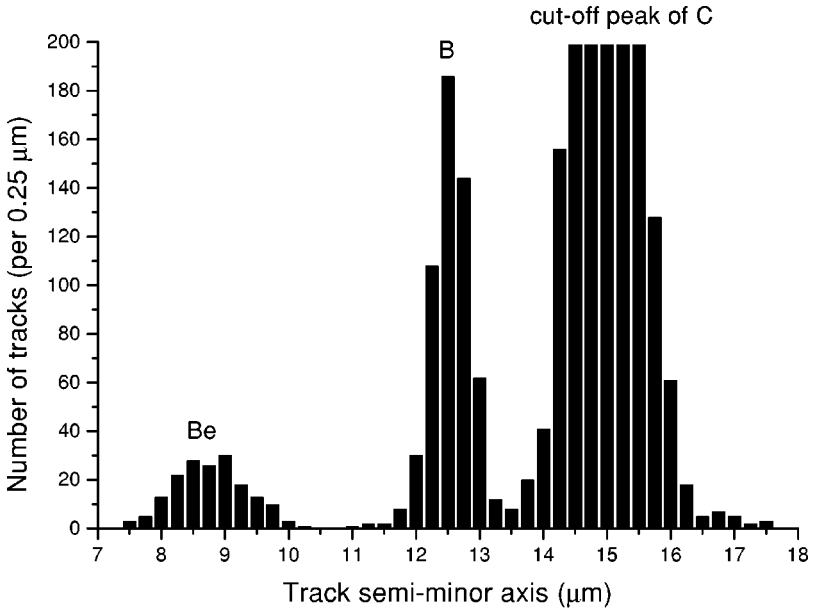

FIG. 1. Track spectrum measured at a depth of 2.2 cm in the paraffin stack. The energy of the beam at the exit of the target is $\sim$253 MeV/nucleon.

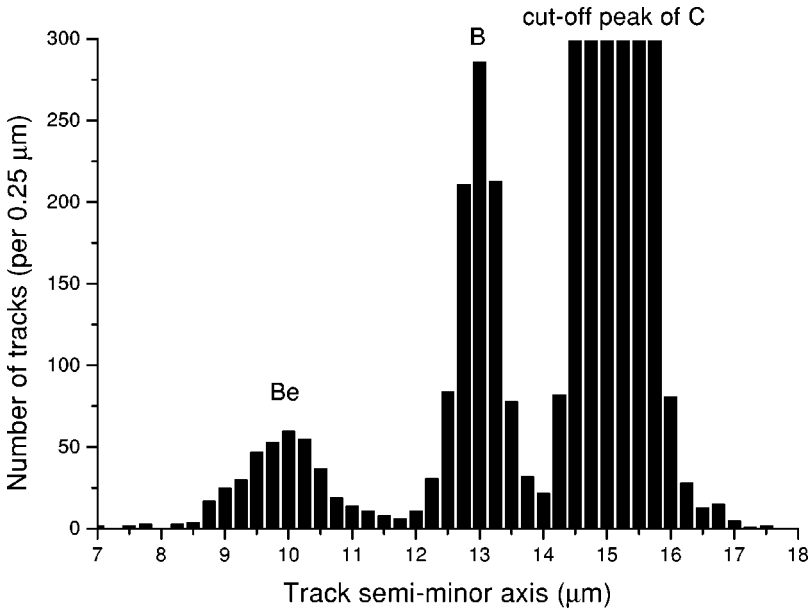

FIG. 2. Track spectrum measured at a depth of 5.5 cm in the water stack. The energy of the beam at the exit of the target is ~207 MeV/nucleon.

here, and those calculated according to two models ($\sigma_{\mathrm{TCC,\,mod}}$) [14,15] for a paraffin target. The latter models account for the energy dependence of the cross section in the considered energy region. Correspondingly, Tables II–IV give all the values of $\sigma_{\mathrm{TCC,\,exp}}$ measured here, those available from prior experiments [9–13] and those obtained from the two models [14,15]. Note that the reaction cross sections from the models were corrected by subtraction of the calculated neutron-removal cross sections according to Sihver *et al.* [14]. We estimated that even if modeled σ_{nr} differ by 50% from that of experiment (i.e. "real σ_{nr}") [17] this would lead to the error in $\sigma_{\mathrm{TCC,mod}}$ [14,15] of ~4%. The energy values (E) in each table are averages of those in front of and behind the target, while the values in parentheses are deviations from these averages. The errors in σ_{TCC} obtained in this work are statistical only and are given in parentheses in the second column from the left. The errors in σ_{TCC} values of previous experiments were taken from the corresponding references. The percentages given in brackets in the last two columns of each table are deviations (Δ) of the present measurements from the model calculations. They are defined as follows:

$$\Delta = \frac{\sigma_{\mathrm{TCC,\,exp}} - \sigma_{\mathrm{TCC,\,mod}}}{\sigma_{\mathrm{TCC,\,exp}}}. \tag{3}$$

Note that $\sigma_{\mathrm{TCC,\,mod}}$ are averages inside the target calculated as

$$\sigma_{\mathrm{TCC,\,mod}} = \frac{1}{E_{\mathrm{in}} - E_{\mathrm{out}}} \int_{E_{\mathrm{out}}}^{E_{\mathrm{in}}} \sigma_{\mathrm{TCC,\,mod}}(E)\,dE. \tag{4}$$

One can see in Figs. 3 and 4 and Tables II–IV that, except for a few results, the values of σ_{TCC} measured here and the results obtained by other groups are consistent within experimental errors. Even when this is not the case, the disagreement is rather small. The semiempirical model reported in Ref. [14] underestimates the present results by 9.9%, 12.3%,

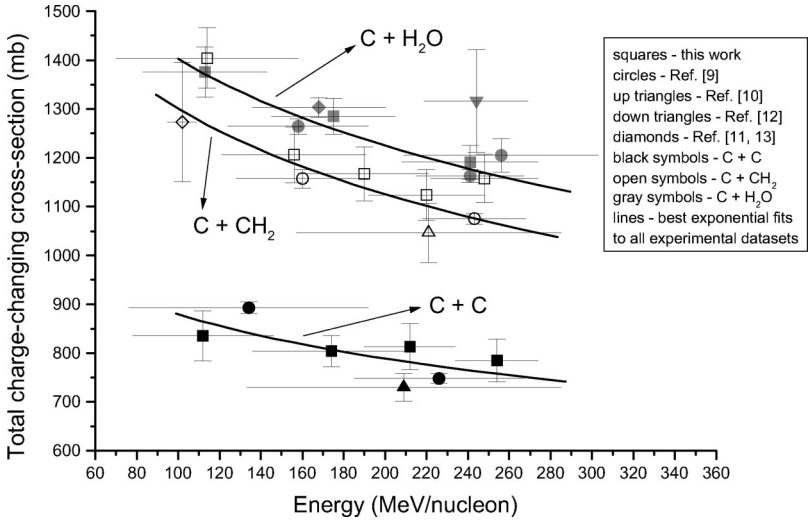

FIG. 3. Total charge-changing cross sections ($\sigma_{\mathrm{TCC,\,exp}}$) obtained in this work in comparison with prior experimental results for the systems studied. Lines that cross the points indicate the energy of the beam in front of and behind a given target.

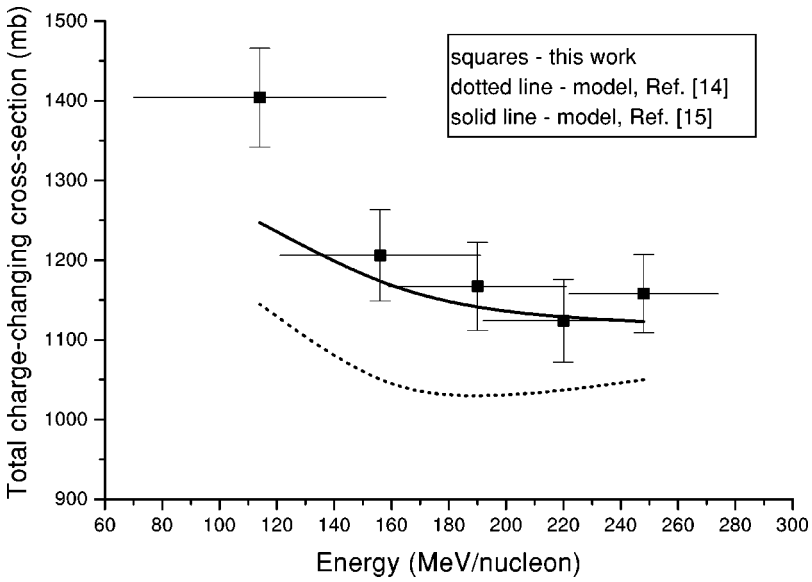

FIG. 4. Total charge-changing cross sections ($\sigma_{\mathrm{TCC,\,exp}}$) obtained here and those calculated according to two models for a paraffin target. Lines parallel to X axis are identical to those of Fig. 3.

and 9.7% on the average for C, CH_2, and H_2O targets, respectively. The empirical model developed at NASA [15] gives results that are closest to the measurements. The deviations of the present experimental results from the model calculations are 1.9%, 4.0%, and 2.4% for C, CH_2, and H_2O targets.

B. Partial cross sections for the production of projectilelike fragments

Use of thick targets (for production of a statistically relevant number of secondary particles) implies that the fragmentation of fragments must be taken into account. Price *et al.* derived a formula [16] applicable for a thick target, assuming that the number of fragments is zero in front of the target and that the total charge-changing cross sections are equal for the primary and secondary particles. Moreover, they estimated that even if σ_{TCC} values differed by as much as 50%, the formula would be correct to within 10%. In the present case, using stacks composed of many detectors and targets, the number of fragments can be large in front of each target. Therefore, the correction to the formula given in Ref. [16] was made. It accounts for the number of fragments in front of the target but still assumes that the σ_{TCC} values are equal for the primaries and secondaries. Indeed, it has been shown experimentally [9] and theoretically [15] that the difference in these σ_{TCC} values for C, B, and Be is negligibly low. Finally, the partial cross section is expressed by (see also Appendix B)

$$\sigma_{\mathrm{PCC}}=\left(\frac{N_{\mathrm{F,\,out}}}{N_{\mathrm{C,\,out}}}-\frac{N_{\mathrm{F,\,in}}}{N_{\mathrm{C,\,in}}}\right)\frac{M}{N_{\mathrm{A}}\rho x}, \tag{5}$$

where $N_{\mathrm{F,\,out}}$ and $N_{\mathrm{F,\,in}}$ are the numbers of fragments measured behind the target and in front of it, respectively. The partial cross sections obtained in this work and in previous experiments (the C beams on the targets used here and previously are of nearly the same beam energies) [11–13,17], and the predictions of different models [14,18–20] are given in Tables V–VII. The presentation of Tables V–VII is identical to that of Tables II–IV. The only difference is the presence of a ΔZ column that gives the charge-loss, i.e., the charge difference between projectile and fragment (1 for a B and 2 for a Be fragment). Note also that the $\sigma_{\mathrm{PCC,\,mod}}$ values now correspond to $\sigma_{\mathrm{PCC,\,mod}}(E)$, since the partial cross-section dependence on energy is weak. In all cases, the values of $\sigma_{\mathrm{PCC,\,mod}}$ were obtained by summing up for all detectable isotopes with $A=11$, 10, 8 for $Z=5$ and $A=10$, 9, 7 for $Z=4$. The $\sigma_{\mathrm{PCC,\,mod}}$ values given in the second column from the right (Ref. [19]) are independent of the projectile energy in the region of $\sim$40–1000 MeV/nucleon. There are not many experimental data concerning carbon ions in the en-

TABLE II. Total charge-changing cross sections from the C +C experiment ($\sigma_{\mathrm{TCC,\,exp}}$) and model predictions ($\sigma_{\mathrm{TCC,\,mod}}$).

E (MeV/nucleon)	$\sigma_{\mathrm{TCC,\,exp}}$ (mb)			$\sigma_{\mathrm{TCC,\,mod}}$ (mb)	
	This work	Ref. [9]	Ref. [10]	Ref. [14]	Ref. [15]
254 (20)	785 (43)			716 [8.8%]	779 [0.8%]
212 (22)	813 (47)	748 (10)	730 (28)	703 [13.5%]	784 [3.6%]
174 (38)	804 (32)			706 [12.2%]	798 [0.7%]
112 (34)	835 (51)	893 (12)		793 [5.0%]	855 [−2.4%]

TABLE III. Total charge-changing cross sections from the C + CH_2 experiment ($\sigma_{TCC,\,exp}$) and model predictions ($\sigma_{TCC,\,mod}$).

E	$\sigma_{TCC,\,exp}$ (mb)				$\sigma_{TCC,\,mod}$ (mb)	
(MeV/nucleon)	This work	Ref. [9]	Ref. [11]	Ref. [12]	Ref. [14]	Ref. [15]
248 (26)	1158 (49)	1075 (11)			1050 [9.3%]	1123 [3.0%]
220 (28)	1124 (52)			1046 (61)	1036 [7.8%]	1128 [−0.4%]
190 (31)	1167 (55)				1027 [12.0%]	1139 [2.4%]
156 (35)	1206 (57)	1157 (19)			1036 [14.1%]	1167 [3.2%]
114 (44)	1404 (62)		1273 (122)		1145 [18.4%]	1247 [11.2%]

TABLE IV. Total charge-changing cross sections from the C + H_2O experiment ($\sigma_{TCC,\,exp}$) and model predictions ($\sigma_{TCC,\,mod}$).

E	$\sigma_{TCC,\,exp}$ (mb)				$\sigma_{TCC,\,mod}$ (mb)	
(MeV/nucleon)	This work	Ref. [9]	Ref. [12]	Ref. [13]	Ref. [14]	Ref. [15]
241 (33)	1191 (35)	1205 (34) 1163 (13)	1316 (105)[a]		1136 [4.6%]	1243 [−4.4%]
175 (30)	1285 (37)	1264 (16)		1303 (20)	1115 [13.2%]	1266 [1.5%]
113 (30)	1376 (52)				1219 [11.4%]	1359 [1.2%]

[a]The value of $\sigma_{TCC,\,exp}$ and its error given in the fourth column from the left were estimated from the fragment yields (the number of fragments with a given Z produced in the target normalized to that of incoming beam particles) and their experimental uncertainties.

TABLE V. Partial charge-changing cross sections from the C + C experiment ($\sigma_{PCC,\,exp}$) and model predictions ($\sigma_{PCC,\,mod}$).

E		$\sigma_{PCC,\,exp}$ (mb)		$\sigma_{PCC,\,mod}$ (mb)			
(MeV/nucleon)	ΔZ	This work	Ref. [17]	Ref. [14]	Ref. [18]	Ref. [19]	Ref. [20]
254 (20)	1	117 (5)	117 (4)[a]	127	104	50	117
	2	40 (3)	39 (10)[a]	54	20	32	38
212 (22)	1	116 (9)		129	102		118
	2	41 (5)		56	21		38
174 (38)	1	122 (8)		130	102		119
	2	44 (5)		59	22		39
112 (34)	1	143 (14)		144	112		121

[a]The errors given in the fourth column from the left are square roots of quadratic sums of experimental uncertainties for each measured isotope, i.e., 12, 11, 10, 8 ($\Delta Z=1$) and 11, 10, 9, 7 ($\Delta Z=2$).

TABLE VI. Partial charge-changing cross sections from the C + CH_2 experiment ($\sigma_{PCC,\,exp}$) and model predictions ($\sigma_{PCC,\,mod}$).

E		$\sigma_{PCC,\,exp}$ (mb)		$\sigma_{PCC,\,mod}$ (mb)			
(MeV/nucleon)	ΔZ	This work	Ref. [11]	Ref. [14]	Ref. [18]	Ref. [19]	Ref. [20]
248 (26)	1	214 (8)		242	233	92	257
	2	74 (5)		105	53	58	77
220 (28)	1	205 (11)		242	234		255
	2	81 (7)		112	55		77
190 (31)	1	206 (14)		242	236		253
	2	80 (8)		119	56		77
156 (35)	1	236 (17)		245	239		254
	2	80 (10)		129	56		77
114 (44)	1	253 (21)	233 (34)	266	247		261

ergy interval of ~110–250 MeV/nucleon and light targets like C, CH_2, and H_2O. Those data available in the literature agree with our results within experimental uncertainties except for one case, which corresponds to $\Delta Z=2$ produced in the reaction of 175 (30) MeV/nucleon C+water [13]. A possible reason for this disagreement could be the fact that, in Ref. [13] the tracks were not matched, and therefore some background events could have been added to the correct number of fragments. Figure 5 shows the deviation of the measured σ_{PCC} values from the model predictions. It is seen that for the systems investigated in this work, the closest values of $\sigma_{PCC,\,mod}$ for $\Delta Z=1$ and 2 are obtained from the NUCFRG2 model [20]. These calculations deviate on an average from the present measurements by only 9 and 5% for B and Be fragments, respectively. Finally, a large discrepancy between our results and the model calculations [14,19] for two and one charge loss is observed and, amounts to 47–58 %, respectively, on average for all the systems used in this work.

IV. CONCLUSIONS

The present method, which uses solid state nuclear track detectors, is a good alternative to electronic detector experiments in providing results that help to improve existing nuclear data bases. The measured cross sections presented here give a realistic picture of the phenomena involved in the transport of light ions through light materials. The accuracy of these values is sufficient to enable a valid comparison with existing models. The total charge-changing cross sections are in a very good agreement (~3%) with the model of Tripathi *et al.* [15]. The fragment production cross sections measured here agree with the previous experiments within experimental error but differences ranging from 5 to 60% appear in the corresponding values from various models. These differences indicate that the models presently available could be improved.

ACKNOWLEDGMENTS

We would like to thank Professor Tripathi from NASA Langley Research Center for providing us with the NUCFRG2 model numbers. A.N.G. acknowledges the financial support of NIRS (Chiba, Japan) during his stay there. J.S., M.G., and R.I. are supported by Research Contract No. PP-0106/99 between the Ministry of Education, Science and Sport of Slovenia and J. Stefan Institute. This work was performed at the NIRS HIMAC facility under Project Number 11P083.

APPENDIX A

Concerning Eq. (2) it should be noted there are no losses of desired events due to scattering outside of the active de-

TABLE VII. Partial charge-changing cross sections from the C + H_2O experiment ($\sigma_{PCC,\,exp}$) and model predictions ($\sigma_{PCC,\,mod}$).

E		$\sigma_{PCC,\,exp}$ (mb)			$\sigma_{PCC,\,mod}$ (mb)			
(MeV/nucleon)	ΔZ	This work	Ref. [12]	Ref. [13]	Ref. [14]	Ref. [18]	Ref. [19]	Ref. [20]
241 (33)	1	210 (6)	202 (11)[a]		254	241	97	212
	2	84 (4)	100 (21)[a]		117	55	61	77
175 (30)	1	225 (10)		232 (21)	255	243		208
	2	76 (6)		115 (18)	133	57		76
113 (30)	1	231 (17)			268	248		215

[a]The values of $\sigma_{PCC,\,exp}$ and their errors shown in the fourth column from the left were estimated from the fragment yields and their uncertainties, respectively.

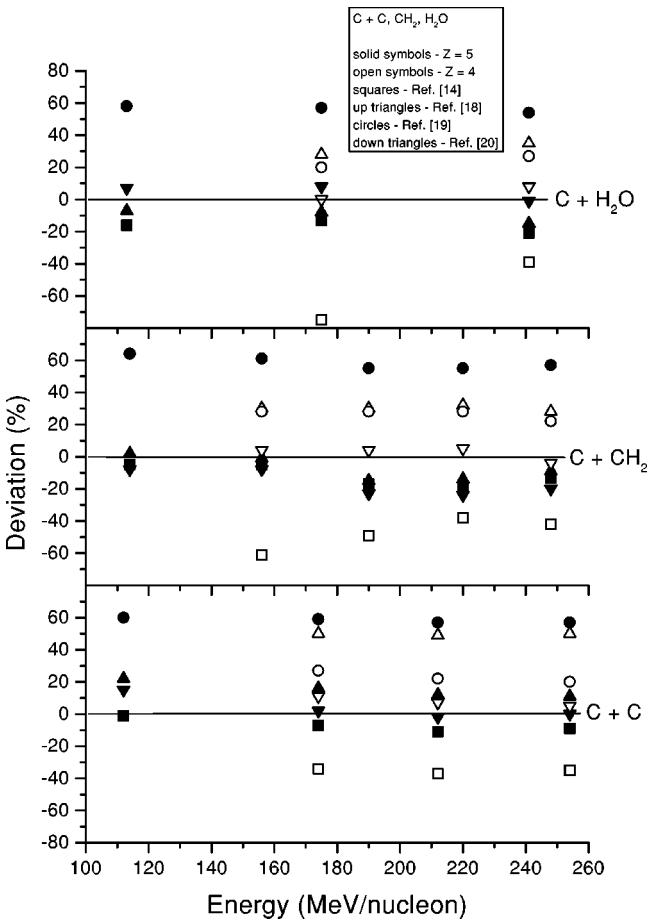

FIG. 5. Deviation of the presently measured cross sections for the production of fragments from those of the studied models.

tector area since it is smaller (by a factor of ~ 1.6) than both the target and the detector. Furthermore the beam density remains almost constant over the whole detector area. This means that the number of particles deflected out of the active area is compensated by an equivalent number of particles deflected into it. We also detect particles that lose neutrons but we cannot distinguish them from the original ^{12}C particles. The ratio of the cross section for production of ^{10}C and ^{11}C isotopes (taken directly from the experiment [17]) to the total charge-changing cross section of ^{12}C on ^{12}C target at 250 MeV/nucleon [17,15] is less than 8%. Moreover, and very importantly, the estimations of the total charge-changing cross section of ^{10}C and ^{11}C particles at 250 and 110 MeV/nucleon on same target according to two models [14,15] differ, as maximum, from that of ^{12}C by 3.2% and 1.2% (at 250 MeV/nucleon), and by 2.7% and 0.8% (at 110 MeV/nucleon). Thus, Eq. (2) is considered to be correct within a few percent in the entire energy region covered in this work.

APPENDIX B

The derivation of the partial cross section, σ_F, follows the assumptions given in Ref. [16] but additionally assumes that fragments exist in front of the target, as discussed in Sec. III B. The target starts at $x=0$, where we have $N_0(0)$ of primary ions and $N_F(0)$ of fragments of given charge. For thick targets we cannot ignore the loss of fragments due to secondary fragmentation but we do ignore the production of fragments of given Z from other fragments. We further assume the same total charge-changing cross section for primary ions and fragments. The number of primary ions decays exponentially as

$$N_0(x)=N_0(0)e^{-(N_A\rho\sigma x)/M}, \tag{B1}$$

where N_A, ρ, and M were defined earlier in the article and σ is the total charge-changing cross section for the primary ions. The change in number of fragments $N_F(x)$ per unit thickness is expressed as

$$\frac{dN_F(x)}{dx}=\frac{N_A\rho\sigma_F}{M}N_0(x)-\frac{N_A\rho\sigma_1}{M}N_F(x), \tag{B2}$$

where σ_1 is the total charge-changing cross section for a given fragment. By inserting Eq. (B1) into Eq. (B2) and solving the differential equation we get

$$N_F(x)=\frac{e^{-(N_A\rho\sigma x)/M}\{-N_0(0)\sigma_F+e^{[N_A\rho(\sigma-\sigma_1)x]/M}[N_F(0)(\sigma-\sigma_1)+N_0(0)\sigma_F]\}}{\sigma-\sigma_1}. \tag{B3}$$

For the case where $\sigma\approx\sigma_1$, we make expansion to the first order of the Taylor series and the Equation (B3) simplifies to

$$N_F(x)=\left(N_F(0)+\frac{N_A\rho\sigma_F x N_0(0)}{M}\right)e^{-(N_A\rho\sigma x)/M}. \tag{B4}$$

It can be mentioned that with the typical values of parameters and variables in our equations ($\rho=1$ g/cm^3, $x=5.5$ cm, $\sigma=800$ mb, $\sigma_F=100$ mb) number of fragments $N_F(x)$ does not change by more than $\pm 2\%$ if σ_1 is within 20% of σ. This is so for the thickest target of 55 mm, the difference is even smaller for thinner targets.

Finally, by taking into account Eq. (B1) the partial cross section is given by

$$\sigma_F=\left(\frac{N_F(x)}{N_0(x)}-\frac{N_F(0)}{N_0(0)}\right)\frac{M}{N_A\rho x}, \tag{B5}$$

where only measured quantities and constants appear.

[1] C-X. Chen *et al.*, Phys. Rev. C **49**, 3200 (1994).
[2] W. Schimmerling, J. W. Wilson, F. A. Cucinotta, and M-H. Y. Kim, NASA STI: 93, International Workshop on Responses to Heavy Ions, Chiba, Japan, 1998, edited by K. Fujitaka *et al.*; http://techreports.larc.nasa.gov/ltrs/ltrs.html
[3] P.L. Petty and A.J. Lennox, Annu. Rev. Nucl. Part. Sci. **44**, 155 (1994).
[4] R. Bimbot, Report Institut de Physique Nucleaire IPNO-DRE-91-27, 1991.
[5] J. Skvarč, Inf. MIDEM **23**, 201 (1993).
[6] J. Skvarč and A.N. Golovchenko, Radiat. Meas. **34**, 113 (2001).
[7] R. P. Henke and E. V. Benton, U.S. Naval Radiological Defense Laboratory (San Francisco) Report USN-RDL-TR-67-122, 1967.
[8] L.R. Gil and A. Marques, Nucl. Instrum. Methods Phys. Res. B **34**, 152 (1998).
[9] I. Schall, D. Schardt, H. Geissel, H. Irnich, E. Kankeleit, G. Kraft, A. Magel, M.F. Mohar, G. Munzenberg, F. Nickel, C. Scheidenberger, and W. Schwab, Nucl. Instrum. Methods Phys. Res. B **117**, 221 (1996).
[10] A. Fukumura, Ph.D. thesis, Tohoku University, Sendai, Japan, 1999.
[11] A.N. Golovchenko, J. Skvarč, N. Yasuda, R. Ilić, S.P. Tretyakova, K. Ogura, and T. Murakami, Radiat. Meas. **34**, 297 (2001).
[12] M. Golovkov, D. Aleksandrow, L. Chulkov, G. Kraus, and D. Schardt, GSI-Preprint-97-08, 1997.
[13] A.N. Golovchenko, J. Skvarč, R. Ilić, L. Sihver, V.P. Bamblevski, S.P. Tretyakova, D. Schardt, R.K. Tripathi, J.W. Wilson, and R. Bimbot, Nucl. Instrum. Methods Phys. Res. B **159**, 233 (1999).
[14] L. Sihver, C.H. Tsao, R. Silberberg, T. Kanai, and A.F. Barghouty, Phys. Rev. C **47**, 1225 (1993).
[15] R.K. Tripathi, F.A. Cucinotta, and J.W. Wilson, Nucl. Instrum. Methods Phys. Res. B **117**, 347 (1996).
[16] P.B. Price, Ren Guoxiao, and W.T. Williams, Phys. Rev. Lett. **61**, 2193 (1988).
[17] J.M. Kidd, P.J. Lindstrom, H.J. Crawford, and G. Woods, Phys. Rev. C **37**, 2613 (1988).
[18] C.H. Tsao, R. Silberberg, A.F. Barghouty, L. Sihver, and T. Kanai, Phys. Rev. C **47**, 1257 (1993).
[19] K. Summerer and B. Blank, Phys. Rev. C **61**, 034607 (2000).
[20] J.W. Wilson, R.K. Tripathi, F.A. Cucinotta, J.L. Shinn, F.F. Badavi, S.Y. Chun, J.W. Norbury, C.J. Zeitlin, L. Heilbronn, and J. Miller, Nucl. Instrum. Methods Phys. Res. B **94**, 95 (1994); NASA TP-3533, 1995, http://techreports.larc.nasa.gov/ltrs/ltrs.html